RSC Advances

ROYAL SOCIETY OF CHEMISTRY

www.rsc.org/advances

Core-Shell ZnSe-CdSe Quantum dots: A facile approach *via* decomposition of cyclohexeno-1, 2, 3-selenadiazole

Sreenu Bhanoth, Priyesh V. More, Aditi Jadhav and Pawan K. Khanna*

For the first time ever cyclohexeno-1, 2, 3-selenadiazole (SDZ) has been employed for the synthesis of core-shell ZnSe-CdSe quantum dots thus promoting an eco-friendly and reasonably less toxic synthesis method for such quantum dots hetero-structure. Synthesized dark-red colored core-shell structures were characterized by UV-Visible and Photoluminescence (PL) spectrophotometer to examine their band-gap. Absorption and emission spectra also showed gradual red-shift in wavelength with respect to zinc selenide (core). Also, band-gap of such core-shell quantum dots can be tuned by varying the shell layer thickness and/or particle size. The findings from the XRD analysis, near-to-homogenous particle size distribution, formation of decent nano-crystalline product and a good agreement with Vegard's law, signifies that the present synthesis approach could be highly effective for the precise tailoring of core-shell QDs.

1. Introduction

Core-shell semiconductor quantum dots are high end research target in nanotechnology including solar cell and light emitting diode applications. Solar energy is most abundant, non-polluting and renewable power resource on the planet. To convert solar energy into electrical energy various photovoltaic devices are employed. Amongst them, silicone solar cell, the first generation solar cell is most utilized device. In silicon solar cell, theoretical maximum conversion efficiency is reported to be 29% and maximum conversion efficiency achieved so far is 24.4%[1]. Silicon solar cells have certain disadvantages such as their high cost of manufacturing, loss of energy as heat due to a large amount of higher energy photons at the blue and violet end of the spectrum and high electron-hole recombination. Further, thin film solar cell i.e. dye sensitized solar cell (DSSC) have shown maximum conversion efficiency of about 11.4% as against theoretically maximum conversion efficiency of 33%[2]. Nano-science and nanotechnology creates a wide scope by using quantum dots sensitized solar cell (QDSSC) to overcome the drawbacks of the conventional solar cells (Silicon and DSSC). Quantum dots sensitized solar cell is one of the potential candidates for third generation low cost solar cell which is likely to be more advantageous due to multi exciton generation and extraction of normalized charge carrier. Maximum theoretical conversion efficiency of QDSSC is described to be 44% which is much higher than DSSC. The achieved maximum conversion efficiency reported so far for QDSSC is 7%[3]. In addition, semiconductor quantum dots have many potential applications in various other fields due to the size and shape dependent absorption that alters the optical property[4]. Core-shell type quantum dot exhibits improved optical properties and are attractive for device technology.

Colloidal core-shell QDs contains at least two semiconductor materials one as the core and other coated on it as a shell, so that the possibility of tuning of their fluorescence wavelength, quantum yield and lifetime can be maintained. In dye sensitized solar cell, dye multi layer reduces performance of the device and the same effect is true for QDSSC[3]. However, core-shell nanocrystals can effectively overcome such problems because it is expected that the shell will create the physical barrier between the cores and surrounding medium, thus making quantum dot surface less sensitive to environmental changes and photo-oxidation. In core shell system the primary purpose of the shell is to create efficient passivation of quantum dot surface to avoid trap states. Recently widely used light harvesting semiconductor quantum dots (QDs) such as CdSe,[4,5,6] PbS,[7,8] CdS [9,10,11,] CdTe[12], InP[13], and Bi_2S_3[14] have been reported for quantum dot sensitized solar cells (QDSSCs). Similarly core-shell QDs e.g. CdSe/CdS, CdS/CdSe[15,16] CdSe/ZnSe[17] CdS/ZnSe[18] CdTe/CdSe[19] CdTe/CdS[20] and CdSe/ZnS[21,22] have found application in QDSSC.

The key step in solar power generation in different types of conventional quantum dot photovoltaic devices such as metal junction solar cells, quantum dot sensitized solar cells (QDSSCs), and polymer hybrid solar cells, is charge separation of the electron and hole[23]. The concept of core-shell quantum dots has been proposed in place of normal QDs for the improvement of both electron and hole carrier transport phenomena. Besides, various possibilities of II-VI compound (ZnSe/CdSe, CdS/CdSe, CdTe/CdSe and CdSe/ZnSe) core-shell QDs semiconductors are considered for such application. In order to fabricate any of these combinations, we need to understand the individual (core/shell) synthesis and characterization of the material.

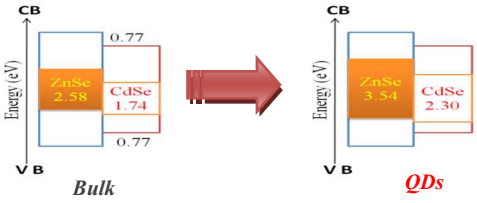

Scheme 1: Band offset in (eV) for interfaces of the bulk and the quantum dot ZnSe-CdSe

The most important property of core-shell semiconducting nanocrystals (CSSNCs) is their core, which emits in visible and near-infrared region of the electromagnetic spectrum due to the quantum confinement effect. Additionally, the 'shell' presence created a passivation around the core thus imparting value to the

optical properties. Due to variation in optical properties, core-shell QDs are important for biomedical applications such as in vitro cell labeling[24,25], in vivo deep cell imaging[26,27] and optical device applications e.g. LEDs[28], lasers[29], phosphors[30]. The typical energy level (band-gaps) of ZnSe core having CdSe shell is depicted in scheme 1.The over-coating of shell of a wide band gap material with narrower band gap materials would open a new route to produce nanocrystals with tunable band gap; the obtained high quality ZnSe-CdSe core-shell semiconductor nanocrystals can have practical application in replacing CdSe QDs as desired emitters. Meanwhile, several groups have attempted synthesis of II-VI and III-V binary semiconductors such as ZnSe/CdSe, ZnO/ZnSe, ZnO/ZnTe, CdSe/CdTe, GaN/GaP and GaN/GaAs[31, 32] with core-shell heterostructures. The methods reported by several researchers are often utilize toxic reagents e.g. phopshines and amines. Mostly these syntheses have been performed by use of trioctylphosphine selenide (TOPSe) as a source of selenium in combination with high boiling solvent. Peter *et al.*[17] described highly luminescent CdSe/ZnSe core-shell nanocrystals by use of CdO, Zinc stearate, trioctylphosphine oxide/hexadecylamine and selenium powder at 250ºC temrature. Similarly, Verma *et al.*[18] reported charge separation by indirect band gap transition in CdS/ZnSe Type-II core-shell quantum dots synthesized by use of cadmium oxide, zinc oxide, oleic acid capping agent, Se powder and octadecene as solvent at 250º C but without addressing the issue of time and energy.

In all above reports, synthesis is carried out by using different Se- pecursors which are highly sensitive, non-eco-friendly, as well as time and energy consuming. Also, there are no reports where 1, 2, 3-selenadiazoles (SDZ) have been employed as a source of selenium for core-shell selenide QDs synthesis despite early reports by the authors of their utility in II-VI semiconductor nanoparticles and quantum dots[33, 34]. The advantage of currently employed organic selenium compound as a source of selenium can be expected from the fact that it releases free selenium when thermolyzed in high boiling solvent (>150 º C) at the same time it avoids use of famous non eco-friendly coordinating reagents such as TOP, TOPO and alkyl amines. In order to make the quantum dots synthesis greener, expected selenium source must be less toxic as well as be able to lower the reaction temperature and

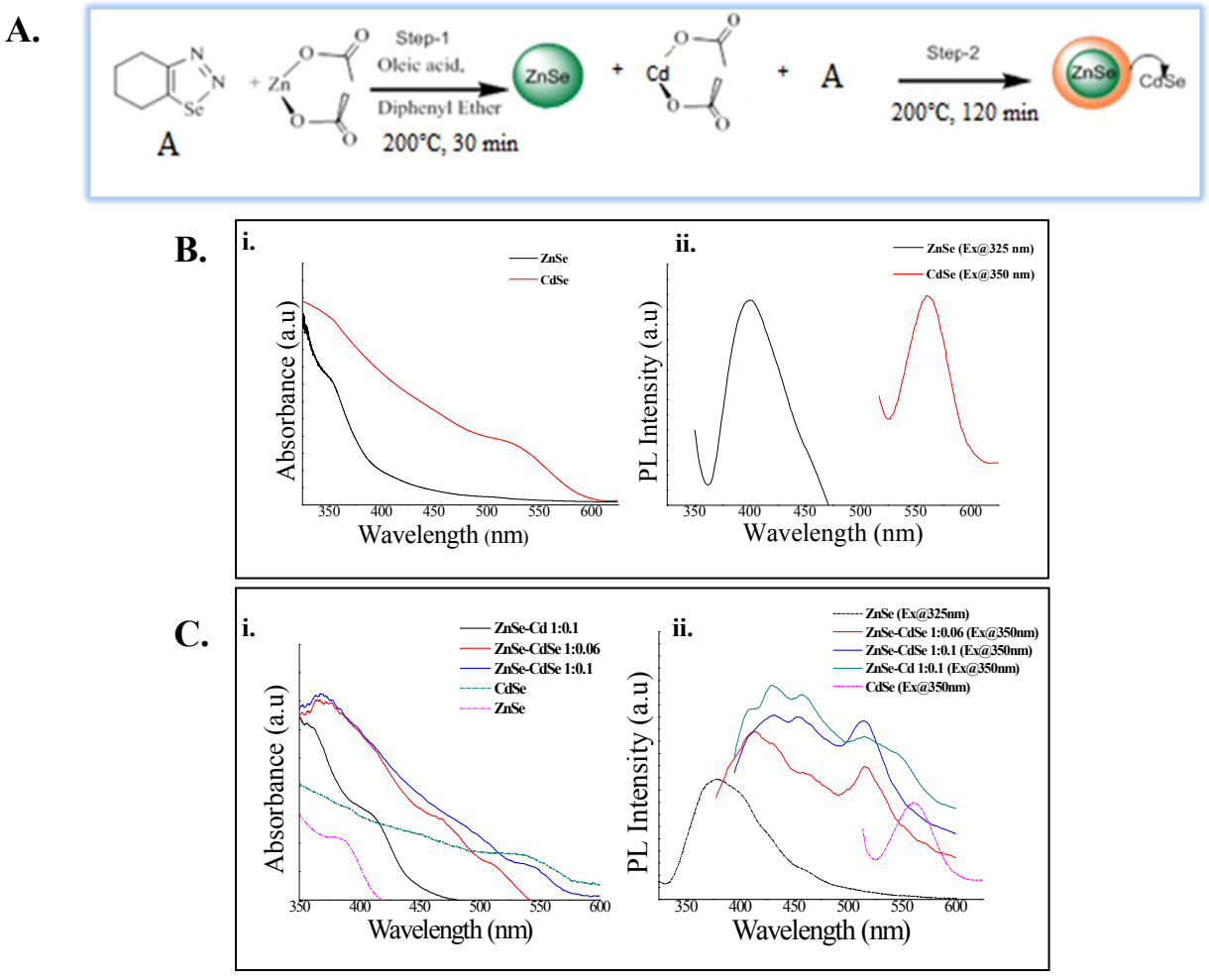

Figure 1: **A)** Typical schematic diagram for synthesis of core-shell quantum dots. **B) i.** UV-Vis. Spectra of ZnSe and CdSe Qds **ii.** PL spectra of ZnSe QDs and CdSe QDs prepared using SDZ and **C)** Monitoring of ZnSe/CdSe core-shell quantum dots during the temporal evolution by **i.** UV-Vis. and **ii.** PL spectra.

time during the preparation. In order to realize this expectation, we herein propose the first use of cyclohexeno-1, 2, 3-selenadiazoles for synthesis of core-shell ZnSe/CdSe quantum dots. Thus this paper describes the synthesis of ZnSe-CdSe and its characterization. Synthesis of core-shell QDs was produced in two steps by using organo-metallic selenadiazole as selenium, cadmium acetate/cadmium oxide as cadmium and zinc acetate as zinc sources respectively and oleic acid as capping agent. Characterization was carried out by using optical absorption spectroscopy, photoluminescence spectroscopy, surface area analyzer, XRD and TEM.

2. Results and Discussion

Based on the earlier reports for synthesis of ZnSe and CdSe QDs[33- 35], nearly mono-dispersed ZnSe core QDs (~2.5 nm size) with absorption onset at 350 nm were first prepared in oleic acid and diphenyl ether media. There after CdSe shell was grown over the ZnSe core template with addition of the Cd and SDZ precursors to the crude ZnSe reactive solution. Upon addition of Cd-precursor to the reactive solution of ZnSe QDs, the colour of solution changes to yellow indicating formation of Cd-layer on ZnSe, further addition of Se precursor leads to the formation of CdSe shell which eventually results in core-shell structure (Figure 1A).

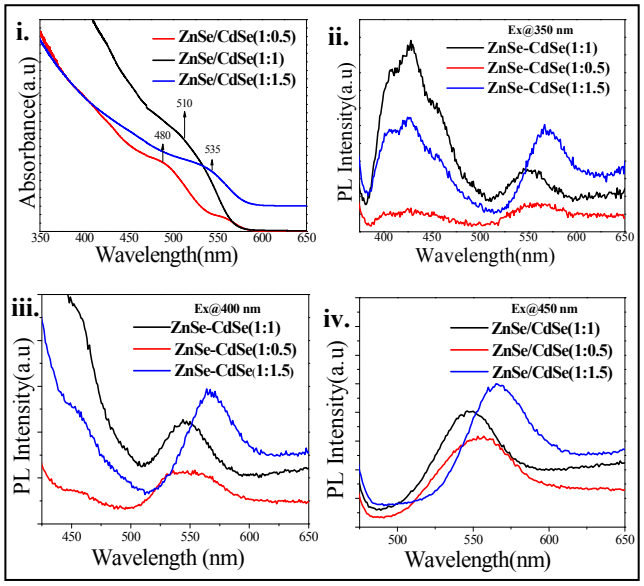

Figure 2: i) UV-Visible spectra of as-prepared re-dispersible core-shell ZnSe-CdSe QDs with different core and shell ratios. **ii)** PL spectra of the core-shell ZnSe-CdSe QDs excited at Ex.350 nm, **iii)** PL spectra of the core-shell ZnSe-CdSe QDs excited at Ex.400 nm and **iv)** PL spectra of the core-shell ZnSe-CdSe QDs excited at Ex.450 nm.

Absorption wavelength of pure ZnSe and CdSe QDs synthesized from the same selenium source (SDZ) showed a band at 350 nm and 540 nm and their emission spectra revealed peaks at 395 nm and 570 nm (Figure 1B ii & 1B iv). During the preliminary synthesis performed to study the temporal evolution of the core-shell combination, formation of core-shell quantum dots and variation of thickness was monitored by UV-Visible spectroscopy (Figure 1B). The experiments were conducted with keeping the ZnSe:CdSe ratios at 1:0.06 and 1:0.1. Another experiment was carried with addition of Cd-source alone to generate Cd-layer on ZnSe core. The ratio of ZnSe:Cd in this case was kept 1:0.1. These preliminary experiments provided the evidence for the size enhancement of CdSe around ZnSe core. The as-prepared core (ZnSe QDs) with the varied CdSe shell thickness showed both the absorption onset and the PL emission peak systematically shifted to the higher wavelength (red-shift). Thus, such considerable red-shift in absorption and emission values indicated the formation of ZnSe-CdSe core-shell structure (Figure 1C). The observed narrow absorption range for ZnSe (core) and red-shift could be due to the band-gap energy of CdSe which lies in the visible region and the combination therefore may be considered more favorable for enhancing the efficiency in light harvesting and quantum dots sensitized solar cell[15]. We purposefully introduced Cd ions by slight addition of Cadmium chloride alone which leads to formation of multiple defect states on the surface of ZnSe core. The ZnSe core served as a matrix to Cd ions which gradually reside on the surface of the ZnSe core. These defects were evident from the emission spectrum of the sample when excited at Ex:350 nm (Figure 1C ii). The fact that Cd atoms were residing at surface of ZnSe core creating surface defects prompted us that the growth of CdSe shell around ZnSe core was feasible. The effect of increasing the CdSe shell layer around ZnSe also showed similar trend in the PL spectra and it appeared from that the PL for ratios of 1:0.06 (ZnSe: CdSe) only predominantly show PL due to ZnSe core but as the shell thickness increases in the ratio 1:0.1, the origin of PL peak is equally dominated by the CdSe shell. Thus, such results hinted towards suppression of PL originated from core with increasing the shell thickness. Such observation correlated well with the fact that ZnSe band-gap is higher than CdSe.

Our efforts to reproduce the experiments to further observe the effect of increased CdSe shell thickness on PL properties resulted in similar results (Figure 2). For this purpose, the experiments were conducted with maintaining the ZnSe:CdSe ratios at 1:0.5, 1:1 and 1:1.5. Thus, overall explanation can be deduced that an excitation at Ex:350 nm results in emission peaks due to both ZnSe core and CdSe shell. The emission from the core was broad between 400-450 nm due to several defect states however it does not change in the emission energy with variation in the shell layer. These results essentially indicated that the ZnSe core was homogeneous in nature and had similar and uniform particle size distribution. However, the observed changes to the PL emission for the core ZnSe with variation in the CdSe shell layer ratio resulted in tunable red shifts when excited at Ex:350nm (broad peak at 450 nm & 555 nm for ratio of 1:0.5 and multiple peaks in the region of 400 -475 nm & a peak at 575 nm for ratio of 1:1.5) as seen in Figure 2 ii. The variation in ZnSe/CdSe ratio should surely lead to difference in shell layer thickness. It was obvious that thinner the shell, higher would be the influence of ZnSe core on the emission wavelength. Similarly, as the shell layer thickness was increased, the influence of CdSe shell increases on the PL properties, inducing the red-shift in the emission wavelength. Such observation was also valid for excitation wavelength of Ex:400 nm and Ex:450 nm (Figure 2 iii & iv).

Table 1: Absorption, Emission wavelength, Band-gap, XRD 2θ value for 111 peak and crystallite size of as-synthesized QDs

S. N	QDs	$\lambda_{(abs.)}$ (nm)	$\lambda_{(em.)}$ (nm) (λ_{EX} @ 325/450 nm)	Bandgap (Eg) (eV)	XRD 2θ value for 111 peak	Crystallite size from Scherer equation	d-spacing (nm)	Lattice constant (a) (nm)
1		350	395	3.54	27.5 [35]	~4 nm	0.3240	0.565
2	ZnSe-CdSe (1:0.5)	480	555	2.58	25.9	~5 nm	0.3436	0.590
3	ZnSe-CdSe (1:1)	510	560	2.21	25.6	~6 nm	0.3476	0.602
4	ZnSe/CdSe (1:1.5)	535	570	2.31	25.4	~7.2 nm	0.3506	0.610
5	CdSe	540	575	2.30	25.3 [34]	~4 nm	0.3516	0.615

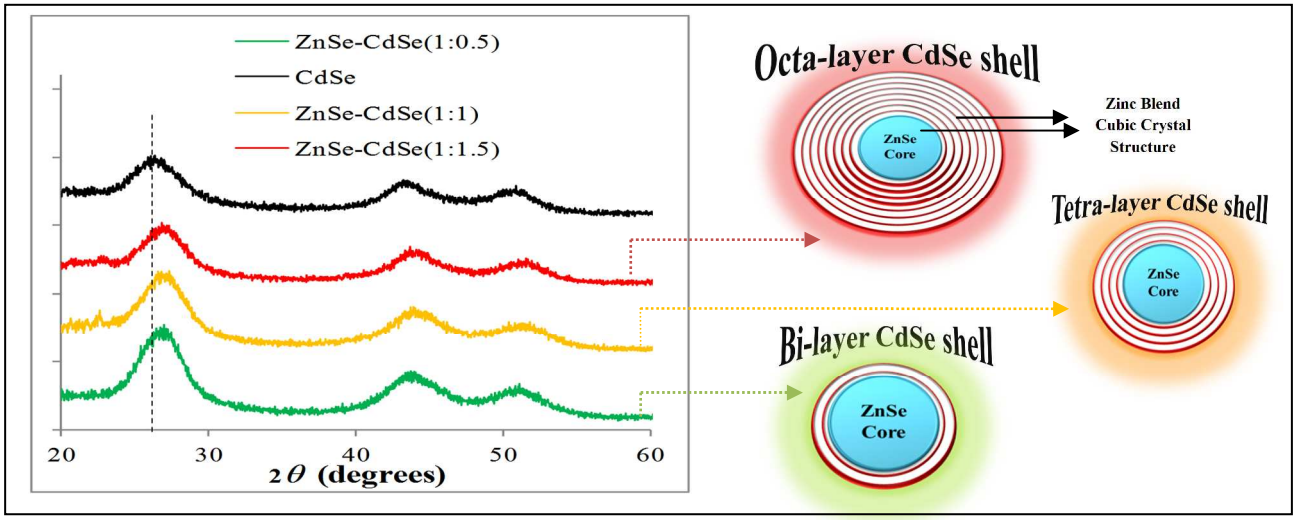

Figure 3: XRD pattern of cubic ZnSe-CdSe quantum dots and schematic representation of bi-, tetra- and octa-layer CdSe shell on ZnSe core with respect to various ZnSe/CdSe ratios.

The Core ZnSe exhibited quantum yield of about 40%. However, the quantum yield of the ZnSe-CdSe core shell quantum dots surprisingly decreased as compared to the core ZnSe quantum dots. The quantum yield of samples with ratio 1:0.5, 1:1 and 1:1.5 (ZnSe:CdSe) was in the order of 4.6%, 5.7% and 8 % respectively. The decrease in quantum yield could be due to the quick burst of growth of CdSe shell around the ZnSe core following the addition of Cd and Se precursors. These observations signaled that the rapid shell growth phase resulted in surface defects and surface disorder, which can be removed by surface relaxation and/or reconstruction during the annealing phase under near-zero growth rates during synthesis[36].

The Bragg's reflections for cubic zinc blend ZnSe had characteristic features at 27.5, 45.6 and 54.3 corresponding to the (111), (220) and (311) planes respectively (Joint Committee on Powder Diffraction Standards, JCPDS, Card No. 80-0021). Similarly, The Bragg's reflections for cubic zinc blend CdSe had characteristic features at 25.3, 42.0 and 42.0 corresponding to the (111), (220) and (311) planes respectively (JCPDS, Card No. 19-0191)[37-38]. The ZnSe-CdSe core shell QDs were expected to show some shifts in the peak patterns, preferably in between the reported peaks for cubic ZnSe and cubic CdSe. This assumption was well justified in the XRD spectra of the ZnSe-CdSe core shell QDs. The XRD measurements (Figure 3) from the powdered samples of ZnSe-CdSe core- shell QDs showed zinc blend cubic crystal structure. The peak position was shifted towards cubic CdSe as the shell thickness was increased. The 2θ values for the sample with the ratio 1:0.5 (ZnSe:CdSe) were observed at 25.9, 42.8 and 50.5 for (111), (220) and (311) planes respectively. These peaks shifted to the 2θ values of 25.6, 42.4 and 50.3 for the sample with the ratio 1:1 for (111), (220) and (311) planes respectively. The shift continued towards zinc blend cubic CdSe for the sample with the ratio of 1:1.5, as the 2θ values were observed at 25.4, 42.1 and 50.1for (111), (220) and (311) planes respectively. Such shifts in the XRD peaks further emphasized the influence of CdSe shell on the ZnSe-CdSe core-shell QDs and correlated well with the findings from the optical properties of the as-synthesized ZnSe-CdSe core-shell QDs[39]. The 2θ values for (111) peak for all the samples are listed in Table 1.

If we consider the present ZnSe-CdSe core-shell QDs as an alloy and consider ZnSe and CdSe as its individual components, the observed dependence of XRD peak positions on the Zn/Cd ratio could be in accordance with the Vegards law.[40]

$$a^{AB}(x) = xa^{A} + (1\text{-}x)a^{B}$$

Where, *A* and *B* are the two semiconductor materials, *'x'* is the alloy composition or the alloy mole fraction of the semiconductor materials and a^{A}, a^{B} are the lattice constant of the respected semiconductor materials. The lattice constants along with d-spacing values for the samples synthesized at different ratios of ZnSe and CdSe were calculated from the XRD spectra and mentioned in the Table 1. The values of lattice constant, d-sapcing and crystallite size showed ordered increase with increasing the ratios of ZnSe:CdSe in the as-synthesized ZnSe-CdSe core shell QDs. These observations from Table 1 allowed u to assume that the as-synthesized ZnSe-CdSe core-shell QDs satisfyingly follow the Vegard's law.

The broadness of the peaks indicates small particle size of the product. The calculated crystallite size from the scherrer's formula was ~5 nm, ~6 nm and 7.2 nm for the samples with the ratio 1:0.5, 1:1 and 1: 1.5 respectively. The increase in crystallite size also confirmed the growth of CdSe shell thickness in the final product as the ratio of CdSe was increased. If we assume that the covalent atomic radius of Cd (144 pm) and Se (120 pm), the approximate size of one CdSe atom would be ~500 pm (including the bond length of CdSe = 230 pm)[41]. Since, the increase in crystallite size for the ZnSe:CdSe ratio of 1:0.5 was 1nm as compared to the core ZnSe quantum dot particle. There could be a bi-layer of CdSe shell formed on the ZnSe core, as there was a possibility of only two CdSe atom stacked above each other in the shell thickness of 1 nm.

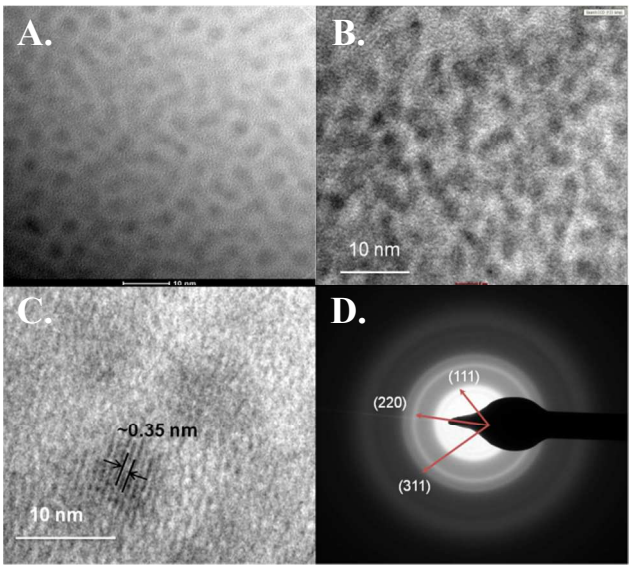

Figure 4: **A)** TEM image of oleic acid capped of ZnSe-CdSe core shell QDs with ratio (1:1.5) (scale bar 10 nm), **B)** CdSe quantum dots synthesized from SDZ, **C)** TEM image of ZnSe-CdSe core shell QDs with ratio (1:1.5) showing clear lattice fringes and **D)** SAED image of ZnSe-CdSe core shell QDs with ratio (1:1.5) showing poly crystalline nature of the QDs.

Thus, we could assume, for every 1 nm increase in the crystallite size of the ZnSe-CdSe core-shell thickness, there could be two layers of CdSe atoms formed in the shell i.e. tetra-layer and Octa-layer CdSe shell for product synthesised with a ZnSe:CdSe ratio of 1:1 and 1:1.5 respectively. In addition, the low intensity peaks (for crystal planes 400, 422 and 331) was also seen in the XRD pattern. The observation of such peaks beyond 2θ value of 60º often indicates well nano-crystalline nature of the sample. (SI. Figure 1). The findings from the XRD analysis and a good agreement with Vegard's law, signifies that the present synthesis approach could be highly effective for the precise tailoring of core-shell QDs.

High-quality of non-agglomerated QDs of ZnSe-CdSe showed spherical particles when analyzed by transmission electron microscopy (TEM). TEM analysis of CdSe alone as shown in Figure 4A showed slightly aggregated spherical particle of about 4-5 nm with white patches around indicating the presence of organics. However, TEM image of ZnSe-CdSe core-shell QDs (Figure 4B) with a ratio of 1:1.5 (ZnSe:CdSe) revealed spherical particles with size of more than 5 nm (~7-8 nm) with neat lattice fringes (Figure 4C). The crystalline nature of the particles was also confirmed from the single area electron diffraction (SAED) pattern (Figure 4D) and the d-spacing measured from the lattice fringes for the sample with 1:1 ratio correlated well with the XRD findings. The TEM images further confirmed the nano-crystlline behaviour of the as-synthesized core-shell QDs along with the increase in particle size with increase in CdSe shell.

Dynamic scattering technique (DLS) method was utilized to calculate the particle size distribution within a given colloidal solution. In the present case, the core-shell QDs synthesized with the ratio of (1:1.15) were dissolved in toluene and the analysis by an action of Laser scattering of wavelength 632 nm revealed that the tiny core-shell nanostructures were narrowly distributed within 6 nm (SI. Figure 2). The obtained narrow particle distribution could be attributed to excellent size quantization effect in the ZnSe-CdSe core-shell quantum dots. The TEM analysis coupled with DLS also confirmed the homogeneous particles size in the sample.

3. Conclusions

To conclude, we have demonstrated the use of cyclohexeno-1, 2, 3-selenadiazole for the first time to synthesize ZnSe-CdSe core/shell quantum dots and large scale (gram-level) production was also successfully attempted. Detailed study was performed to observe the temporal evolution of the core-shell combination and formation of core-shell quantum dots with variation of shell thickness. Systematic red shift was observed from the optical spectroscopy (UV-visible and PL) as the shell thickness was increased varying the concentrations of CdSe in the final product. The findings from the XRD analysis, near-to-homogenous particle size distribution, formation of decent nano-crystalline product and a good agreement with Vegard's law, signifies that the present synthesis approach could be highly effective for the precise tailoring of core-shell QDs.

4. Experimental

Materials and methods

Cyclohexeno-1, 2, 3-selenadiazole (SDZ) was synthesized by the earlier reported method[33]. Freshly prepared SDZ was used for the experiments while rest of the SDZ was stored under dark conditions to avoid the decomposition from sunlight. Oleic acid (99%) and Diphenyl ether (99%) (Sigma-Aldrich Co), Acetone

and Zinc acetate (98%) (Mark (I) Ltd, Cadmium acetate (98%) (Qualigens (I) Ltd.), Methanol and hexane (Alfa Aesar), were purchased commercially. All chemicals were used as received.

Progress of reaction was monitored via temporal evolution of bands using high power xenon light source UV-Visible spectrophotometer, Ocean Optics US Florida (Makropack) by scanning the samples between 325 nm-650 nm in toluene solution. The absorption spectra of the as-prepared quantum dots were measured by same technique. Photoluminescence (PL) of various stages of reaction as well as of final products was recorded using Eclipse fluorescence spectrophotometer (Agilent Technologies) at varied excitation wavelength *viz*; 350, 400 and 450 nm depending upon the nature of samples. X-ray diffractions patterns were measured by using Cu-Kα (λ=1.5406Aº) radiation having tube voltage with 40mA current on Mini Flex Rigaku X-ray diffractrometer. XRD pattern was recorded in the angular range $2º < 2\Theta < 90º$. Thus, cubic crystal phase of quantum dots was established by XRD by Size of the quantum dot examined directly by Techni-20 transmission electron microscopy (TEM) and 200 KeV acceleration voltage was used for the experiment. Particle size distribution was measured for toluene solution in the range of 0-100 nm using Sympatech (France) particle size analyzer at a Laser wavelength of 632 nm.

The PL quantum yield for both ZnSe core and ZnSe-CdSe core-shell quantum dots was obtained by referring to a standard (Rhodamine 6G, QY=95%). The PL quantum yield was calculated using the following equation[42].

$$\phi = \phi' \times (I/I') \times (A'/A) \times (n/n')^2$$

Synthesis of CdSe Quantum dots:

CdSe QDs were synthesized as per reported proceudre[34]. Typically, cadmium acetate (0.8 g) and oleic acid (10 ml) was placed in 250 ml three-necked flask and was heated for an hour at ~100ºC under nitrogen atmosphere. Diphenyl ether (30 ml) was added to this reaction mixture at the same temperature followed by drop-wise addition of cyclohexeno-1, 2, 3-selenadiazole (0.65 g) in diphenyl ether over a period of 10-15 min. The reaction mixture was then heated to about 200 ºC and the reaction was maintained with stirring at this temperature for 2-3 hours. Reaction suspension was there after cooled to room temperature followed by addition of hexane (50 ml) and ethanol (40-50 ml) for an overnight ageing and precipitation of the QDs. Finally the product was collected by centrifugation and dried in an oven at 60 ºC for 2-4 hours.

Synthesis of ZnSe Quantum dots

Synthesis of ZnSe quantum dots was performed by the previously reported method[35]. Typically, Zinc acetate (1.0 g) and oleic acid (15 ml) was placed in three-necked flask (250 ml) and was refluxed for an hour at ~180ºC under nitrogen atmosphere Diphenyl ether (30 ml) was added to this reaction mixture at the same temperature followed by drop-wise addition of cyclohexeno-1, 2, 3-selenadiazole (0.65 g) in diphenyl ether over a period of 10-15 min. The reaction mixture was then heated to about 200 ºC and the reaction was maintained with stirring at this temperature for 2-3 hours. Reaction suspension was there after cooled to room temperature followed by addition of hexane (50 ml) and ethanol (40-50 ml) to precipitate the final product. The reaction mixture was left overnight to complete aging process. Finally the end product was collected by centrifugation and dried in an oven at 60 ºC for 2-4 hours.

Synthesis of core-shell ZnSe-CdSe use of cyclohexeno-1, 2, 3-seleandiazole:

The synthesis of core-shell ZnSe-CdSe was conducted by adding Zinc acetate (1.0 g) and oleic acid (20 ml) in three-necked flask (250 ml) and the mixture was refluxed for an hour at about 180ºC. Diphenyl ether (35 ml) was then added to the flask at the same temperature. Subsequently, diphenyl ether solution of cyclohexeno-1, 2, 3-selenadiazole (0.62 g) was added drop-wise to the reaction mixture and the temperature was raised to ~200 ºC. The reaction was performed with rapid stirring for 30 min after which it was cooled to about 150-160º C for second stage. For generating CdSe shell around the ZnSe core (1:1 ratio), cadmium acetate (1.5 g) or cadmium oxide (0.75 g) and cyclohexeno-1, 2, 3-selenadiazole (0.65 g) were added to the same reaction mixture as mentioned above, and the reaction was continued for another two hour at ~200ºC. After this period, the heating was discontinued and the solution was allowed to cool to 50-60º C. Later, hexane and ethanol (50 ml each) was added and the mixture was further stirred for 10-20 min. The reaction mixture was left overnight for aging process. Finally, red colored core-shell quantum dots of ZnSe-CdSe were collected by centrifugation and dried in an oven at 60ºC for 2-4 hours. These were completely re-dispersible in toluene and hexane. Similarly, ZnSe core with CdSe shell with 1: 0.5 and 1: 1.5 ratios were synthesized by varying the shell precursor.

5. Acknowledgment

PKK acknowledges the Funding by DST, Govt. of India, New Delhi. Authors thank Dr. Prahlada, Vice chancellor of DIAT (DU) for encouragement and financial support to SB.

Notes and references

* *Corresponding author Email: pawankhanna2002@yahoo.co.in*
Nanochemistry/Nanomateirals Lab., Dept of Applied Chemistry, Defence Institute of Advanced Technology (DIAT), Govt. of India, Pune - 411 025, India.

† Electronic Supplementary Information (ESI) available: 1) XRD spectra of the various as-synthesized ZnSe-CdSe core-shell QDs and 2) the particle size distribution data of the the core-shell QDs synthesized with the ratio of (1:1.15) obtained from dyanamic laser scattering technique by an action of Laser scattering of wavelength 632 nm.

1. Z. Jianhua, W. Aihua, , A. G.Martin, F. Francesca, *Appl. Phys. Lett.*, 1998, **73**, 1991.
2. H. Liyun. I. Ashraful, H. Chen, M. Chandrashekaram; B. Chiranjeevi, Z. Shufang, Y. Xudong, Y. Masatoshi; *Energy Environ. Sci.*, 2012, **5**, 6057.
3. H. I. Alexander, S. M. Susana, H. Sjoerd, V. Oleksandr, Z. David, D. Ratan, L. Larissa, R. R. Lisa, H. C. Graham, F. Armin, W. K. Kyle, J. K. Illan, N. Zhijun, J. L. Andre, W. C. Kang, M. Aram and H. S. Edward, *Nature Nanotechnology*, 2012, **7**, 577-582.
4. I. Robel, V. Subramanian, M. Kuno, P. V. Kamat, *J. Am. Chem. Soc.*, 2006, **128**, 2385-2393.

5. J. Chen, W. Lei, W. Q. Deng, *Nanoscale*, 2011, **3**, 674-677.
6. 6. Kongkand, A.; Tvrdy, K.; Takechi, K.; Kuno, M.; Kamat, P.V., *J. Am. Chem. Soc.*, **2008**, *130*, 4007-4015.
7. B. R. Hyun, Y. W. Zhong, A. C. Bartnik, L. Sun, H. D. Abruna, F. W. Wise, J. R. Goodreau, J. R. Matthews, T. M. Leslie, N. F. Borelli, *ACS Nano*, 2008, **2**, 2206-2212.
8. H. C. Leventis, F. O'Mahony, J. Aktar, M. Afzal, P. O'Brien, S. A. Haque, *J. Am. Chem. Soc.*, 2010, **132**, 2743-2750.
9. P. A. Sant, P. V. Kamat, *Phy. Chem. Chem. Phy.,* 2002, **4**, 198-203.
10. W. Sun, Y. Yu, H. Pan, X. Gao, Q. Chen, L. Peng, *J. Am. Chem. Soc*., 2008, **130**, 1124-1125.
11. D. R. Baker, P. V. Kamat, *Adv. Funct. Mater*, 2009, **19**, 805-811.
12. Z. Yang, C. Y. Chen, C. W. Liu, C. L. Li, H. T. Chang, *Adv. Energy Mater*, **2011**, *1*, 259-264.
13. A. Zban, O. I. Micic, B. A. Gregg, A. J. Nozik, *Langmuir*, 1998, **14**, 3153-3156.
14. L. M. Peter, K.G.U. Wijayntha, D. J. Riley, J. P. Waggett, *J. Phy. Chem, B*., 2003, **107**, 8378-8371.
15. Z. Pan, H. Zhang, K. Cheng, Y. Hou, J. Hua, X. Zhong, *ACS Nano*, **2012**, *6(5),* 3982-3991.
16. Y. Zusing, Y. Chia, L. Chi-Wei, C. Huan-Tsung, *Chem. Commun.*, 2010, **46**, 5485-5487.
17. R. Peter, B. Joel, P. Adam, *Nano Lett*., 2002, **2***,* 781-784.
18. S. Verma, K. Sreejith, N. G. Hirendra, *J. Phy. Chem. C*., 2013, **117,** 10901−10908.
19. C. Chi-Hung, S. L. Shun, D. S. Gregory, B. Clemens, *J. Phys. Chem. Lett*, 2010, **1**, 2530-2535.
20. Y. Yueran, G. Chen, P. Gregory Van Patten, *J. Phy. Chem. C*., 2011, **115**, 22717-22728.
21. J. B. Sambur. B. A. Parkinson, *J. Am. Chem. Soc.*, 2010, **132**, 2130-2131.
22. I. Robel, M. Kuno, P. V. Kamat, *J. Am. Chem. Soc*., 2007, **129**, 4136-4137.
23. K. Wang, J. Chen, W. Zhou, Y. Zhang, Y. Yan, J. Pern, A. Mascarenhas, *Adv. Mater.*, **2008**, *20*, 3248-3253.
24. J. M. Klostranec, W. C. W., Chan, *Adv. Mater*, 2006, **18**, 1953-1964.
25. I. L. Medintz, H. T. Uyeda, E. R.Goldman, H. Mattoussi, *Nat. Mater.*, 2005, **4**, 435-446.
26. J. Shan, H. Yanxi, Z. Zhanjun, L. Lei, H. Hai-Chen, *Journal of Nanomaterials,* 2011, **1**, 1-13.
27. T. Pellegrino, S. Kudera, T. Leidl, A. M. Javier, L. Manna, W. Parak, *Small,* 2005, **1***,* 48-63.
28. S. Qingjiang, Y. A.Wang, L. Li Song, D. Wang, T. Zhu, J. Xu, C. Yang, Y. Li., *Nature Photonics*, 2007, **1**, 717-722.
29. V. I. Klimov, S. A. Ivanov, J. Nanda, M. Achermann, I. Bezel, J. A. McGuire, A. Priyatinski, *Nature*, 2007, **447**, 442-466.
30. J. Lee, V. C. Sunder, J. R. Heine, M. G. Bawendi, J. F.Jensen, *Adv. Mater*, 2006, **18**,1953-1964.
31. Y. Zhang, L. W. Wang, A. Mascrenhas, *Nano. Lett*, 2007, **7***,* 1264–1269.
32. J. Schrier, D. O. Demchenko, L. W. Wang, L. W. Alivisatos, *Nano Lett.*, 2007, **7**, 2377-2382.
33. H. Meier, E. Voigt, *Tetrahedron*, 1972, **28**, 187-192.
34. R. K. Beri, P. K. Khanna, *J. Nanosci. Nanotech*., 2011, **11**,5137-5142.
35. P. K. Khanna, P. More, R.Shewate, A. K. Viswanath, V. Singh, and B. R. Mehta, *Chemistry Letters*, 2009, **38**, 676-77.
36. R. K. Beri, P. More; B. G. Bharate, P. K. Khanna, *Current Applied Physics*, 2010, **10**, 553-556.
37. Z. T. Deng, L. Cao, F. Q. Tang, B. S. Zou; *J. Phys. Chem. B*, 2005, 109,16671–16675.
38. Y. G. Zheng, Z. C. Yang, J. Y. Ying, *Adv. Mater.,* 2007, **19**, 1475–1479.
39. Deng. Z, Lie F., Shen S., Ghosh I., Mansuripur M., and Muscat A. J., *Langmuir,* 2009, **25**, 434-442.
40. L. Vegard, H. Schjelderup, *Z. Phys.,* 1917, **18**, 93-96.
41. S-Y. Chung, L. Sungyul, C. Liu and D. Neuhauser, *J. Phys. Chem. B*, 2009, **113**, 292–301.
42. B. Valeur; Molecular Fluorescence: Principles and Applications, *Wiley-VCH: NewYork*, 2001.

Graphical Abstract